USP19 deubiquitinating enzyme inhibits muscle cell differentiation by suppressing unfolded-protein response signaling

Benjamin Wiles[a,b,c,*], Miao Miao[a,b,*], Erin Coyne[a,b,c], Louise Larose[a,b], Andrey V. Cybulsky[b], and Simon S. Wing[a,b,c]

[a]Polypeptide Laboratory; [b]Department of Medicine, and [c]Department of Biochemistry, McGill University and McGill University Health Centre Research Institute, Montreal, QC H3A OC7, Canada

ABSTRACT **The USP19 deubiquitinating enzyme modulates the expression of myogenin and myofibrillar proteins in L6 muscle cells. This raised the possibility that USP19 might regulate muscle cell differentiation. We therefore tested the effects of adenoviral-mediated overexpression or small interfering RNA (siRNA)-mediated silencing of either the cytoplasmic or endoplasmic reticulum (ER)-localized isoforms of USP19. Only the ER-localized isoform of USP19 (USP19-ER) modulated myoblast fusion as well as the expression of myogenin and myofibrillar proteins, and these effects were also dependent on USP19 catalytic activity. USP19-ER inhibited muscle cell differentiation and the induction of CHOP, a transcription factor in the unfolded-protein response (UPR) that is activated during differentiation. Inducing the UPR by creating mild ER stress with thapsigargin was able to reverse the defect in myoblast fusion caused by the overexpression of USP19-ER, suggesting strongly that USP19 exerts its effects on fusion through its effects on UPR signaling. USP19 also functions similarly in vivo, as USP19$^{-/-}$ mice display improved muscle regeneration concomitant with enhanced expression of CHOP. Collectively these results implicate a deubiquitinating enzyme as a regulator of the UPR. They also suggest that inhibition of USP19 may be a therapeutic approach for the enhancement of muscle growth following injury.**

Monitoring Editor
Jeffrey L. Brodsky
University of Pittsburgh

Received: Aug 12, 2014
Revised: Dec 22, 2014
Accepted: Dec 24, 2014

INTRODUCTION

Muscle wasting is an important complication of aging as well of many diseases such as cancer, heart failure, sepsis, chronic obstructive pulmonary disease, and renal failure. The weakness caused by the muscle wasting decreases the quality of life and, when severe, results in death. The decrease in muscle mass is usually ascribed to atrophy of the myofibers arising from decreased protein synthesis and activated protein degradation (reviewed in Schiaffino *et al.*, 2013). The ubiquitin proteasome system (UPS) is consistently activated in atrophying muscle. In particular, two ubiquitin ligases, MuRF1 (Trim63) and MAFbx/Atrogin-1 (FbxO32) (Bodine *et al.*, 2001; Gomes *et al.*, 2001) appear important in this process. They are up-regulated in various forms of skeletal muscle wasting, and their inactivation results in less muscle loss in response to denervation (Bodine *et al.*, 2001), confirming their importance in mediating muscle atrophy.

Although previous work has emphasized the role of negative protein balance in myofiber atrophy in determining muscle wasting, altered myonuclear dynamics could also play a role in the muscle loss (reviewed in Siu, 2009; Brooks and Myburgh, 2014). A loss of myonuclei has been reported to occur concomitantly with disuse atrophy of the myofibers (Allen *et al.*, 1997). Similarly, recovery from wasting is not only due to net positive protein balance but may also involve myogenesis. During postnatal myogenesis, satellite stem cells in the muscle become activated and undergo both proliferation and differentiation. Muscle differentiation is regulated by a

This article was published online ahead of print in MBoC in Press (http://www.molbiolcell.org/cgi/doi/10.1091/mbc.E14-06-1129) on January 7, 2015.

*These authors contributed equally to this work.

Address correspondence to: Simon S. Wing (simon.wing@mcgill.ca).

Abbreviations used: ANOVA, analysis of variance; CHOP, CCAAT/-enhancer-binding protein homologous protein; CTX, cardiotoxin; DAPI, 4′,6-diamidino-2-phenylindole; DMSO, dimethyl sulfoxide; ER, endoplasmic reticulum; ERAD, ER-associated degradation; FBS, fetal bovine serum; GFP, green fluorescent protein; KO, knockout; MHC, myosin heavy chain; PBS, phosphate-buffered saline; qPCR, quantitative real-time PCR; siRNA, small interfering RNA; TA, tibialis anterior; Tg, thapsigargin; TMD, transmembrane domain; UPR, unfolded-protein response; UPS, ubiquitin proteasome system; WT, wild type.

superfamily of basic helix–loop–helix transcription factors, referred to as myogenic regulatory factors, consisting of MyoD, Myf-5, myogenin, and MRF4 (reviewed in Bentzinger *et al.*, 2012). Induction of Myf-5 and MyoD results in differentiation of satellite cells into myoblasts (Rudnicki *et al.*, 1993). Subsequently myogenin and MRF4 are induced, which results in fusion of myoblasts and maturation of multinucleated myotubes (Hasty *et al.*, 1993). The UPS has also been shown to regulate myogenesis. Pax3, a transcription factor with an important role in embryonic myogenesis, is regulated by the ubiquitin ligase Taf1. Taf1 associates directly with and ubiquitinates Pax3, resulting in its degradation by the proteasome (Boutet *et al.*, 2010). MyoD (Tintignac *et al.*, 2005) and myogenin (Jogo *et al.*, 2009) can also be degraded by the UPS.

Although much attention has been given to the study of ubiquitin ligases in muscle wasting and muscle differentiation, relatively little is known about the roles of deubiquitinating enzymes. Because deubiquitinating enzymes remove ubiquitin from substrates, they are also likely to be important in controlling ubiquitination in skeletal muscle. Our laboratory identified the USP19 deubiquitinating enzyme, and we and others found it to be induced in various conditions of atrophy in rodent skeletal muscle, including fasting, diabetes, dexamethasone treatment, cancer, and denervation (Combaret *et al.*, 2005; Liu *et al.*, 2011; Ogawa *et al.*, 2012). Depletion of USP19 in L6 muscle cells results in increased expression of myofibrillar proteins consistent with a role of this enzyme in promoting catabolism (Sundaram *et al.*, 2009). Structurally, USP19 is expressed as two major isoforms; one with and the other without a C-terminal transmembrane domain (TMD), which confers endoplasmic reticulum (ER) membrane localization with the active site facing the cytosol (Hassink *et al.*, 2009). These two isoforms (herein referred to as USP19-CYT and USP19-ER) arise from differential splicing of the last exon of the gene. USP19 is up-regulated upon induction of ER stress, and overexpression of USP19-ER appears to rescue substrates from ER-associated degradation (ERAD; Hassink *et al.*, 2009). However, silencing of USP19 has an effect on degradation of one (Nakamura *et al.*, 2014) but not other (Lee *et al.*, 2014) substrates, and so the role of USP19 in ERAD remains unclear.

Our previous observations that silencing USP19 induced expression of myofibrillar proteins as well as myogenin in muscle cells suggested that USP19 might modulate muscle cell differentiation. Therefore we decided to determine whether USP19 is involved in and regulated during this process. In addition, we have tested whether specific isoforms of the enzyme are involved in this function. In so doing, we have discovered that deubiquitination by USP19 does modulate muscle cell differentiation and that this function requires the ER-localized isoform and appears to act through regulation of the unfolded-protein response (UPR) signaling.

RESULTS

USP19 expression is up-regulated during muscle cell differentiation in an isoform-specific manner

We first explored whether USP19 was regulated during differentiation of both L6 and C2C12 myoblasts. Total USP19 mRNA levels increased ~3.5-fold during differentiation in L6 myoblasts (Supplemental Figure 1, A and C), while protein levels increased by ~1.5-fold in both L6 and C2C12 cells (Figure 1A and Supplemental Figure 1, B and C). Because alternative splicing of the USP19 gene creates two distinct isoforms (Figure 1B), we explored whether they are differentially regulated during myogenesis. Using isoform-specific primers targeting each isoform's unique C-terminal end, we observed that mRNA transcripts encoding the cytoplasmic isoform (USP19-CYT) showed a more robust up-regulation during differentiation compared with the ER-localized isoform (USP19-ER) (Figure 1C). These findings indicate that USP19 cytosolic and ER-localized

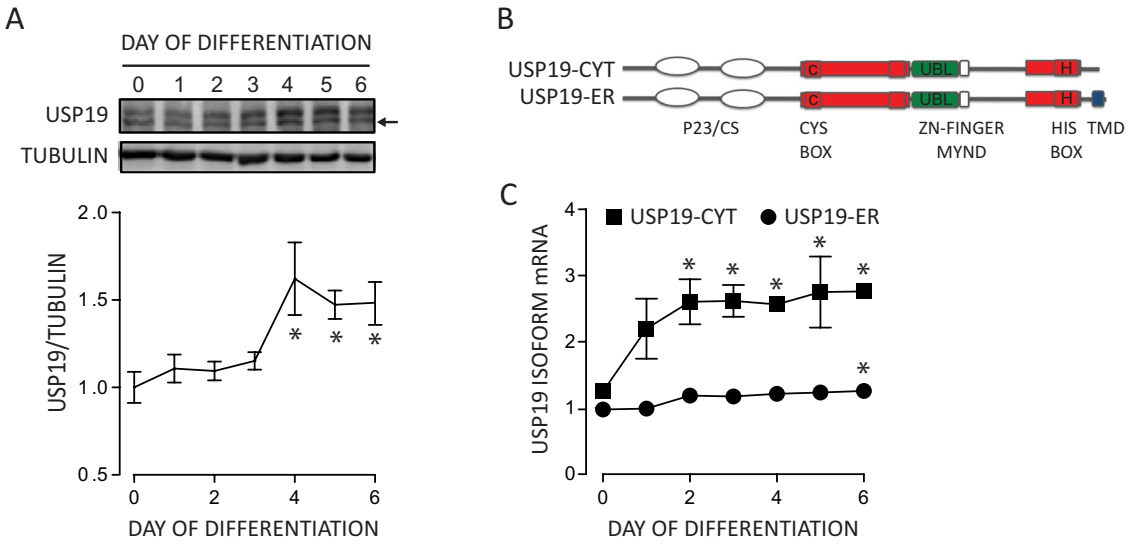

FIGURE 1: USP19 expression is regulated during muscle cell differentiation in an isoform-specific manner. C2C12 myoblasts were plated and induced to differentiate. mRNA and protein from the samples were extracted on the indicated days in differentiation medium. (A) Shown at the top is a representative Western blot of USP19 protein from day 0 to day 6 of differentiation. Arrow identifies a nonspecific band. Shown below is the quantitation of USP19 protein levels ($n = 6$). Shown are means ± SE. *, $p < 0.05$ compared with day 0 (analysis of variance [ANOVA]). (B) Schematic depicting USP19-ER and USP19-CYT isoforms with common structural domains and unique C-terminal domains. The C-terminal TMD confers ER localization to the USP19-ER isoform. (C) Quantitative PCR for USP19 isoforms ($n = 6$). Shown are means ± SE. *, $p < 0.05$ compared with day 0 (ANOVA). Error bars are omitted in instances in which they are smaller than the data point symbol.

isoforms are differentially regulated during muscle cell differentiation and may play distinct roles in this process.

USP19 inhibits fusion of L6 myoblasts and expression of myogenin and major myofibrillar proteins

Because USP19 is induced during differentiation, we tested whether depleting USP19 would adversely affect this process. Surprisingly, silencing of USP19 (by ~80%) resulted in markedly enhanced myotube formation and fusion, the latter measured as the proportion of nuclei that were in myotubes (Figure 2A). For determining whether overexpressing USP19 would have the opposite effect, L6 myoblasts were transduced with adenovirus expressing either USP19-ER or green fluorescent protein (GFP) as a control. Indeed, overexpression of USP19-ER by about fivefold delayed formation of myotubes (Figure 2B). After 48 h of differentiation, cells transduced with adenovirus expressing GFP were ~90% fused, whereas cells overexpressing USP19 were only ~30% fused (Figure 2B). After 72 h of differentiation, the percentage fusion of cells overexpressing USP19 became similar to the GFP control, but the myotubes were thinner and less sheet-like (Figure 2B).

Because we previously showed that the depletion of USP19 increases levels of major myofibrillar proteins as well as the myogenic regulatory factor, myogenin (Sundaram *et al.*, 2009), we tested whether overexpressing USP19-ER would have the opposite effect. Protein levels of myogenin (Figure 2C) and myosin heavy chain (MHC) and tropomyosin (Figure 2D) were indeed decreased by more than 50% upon expressing USP19. These findings confirm that modulation of USP19 levels can regulate fusion and expression of myofibrillar proteins.

USP19 catalytic activity and ER localization are required for inhibition of muscle cell fusion and modulation of myogenin and major myofibrillar proteins

To gain further insights into how USP19 functions, we tested whether these effects were mediated specifically by the USP19-ER isoform and whether its deubiquitinating activity was required. We therefore transduced C2C12 myoblasts with adenovirus expressing either USP19-ER, a catalytically inactive form (with mutation of its active-site cysteine to an alanine [USP19-ER-CA]), USP19-CYT, or GFP as a control. We switched to C2C12 cells to verify that these effects of USP19 were not limited to one muscle cell type as well as to avoid toxicity of adenoviral transduction, which was sometimes seen with L6 cells but not with C2C12 cells. The predicted subcellular localization (cytoplasmic or ER localized) of these adenovirally expressed USP19 isoforms was confirmed by immunofluorescence (IF) and confocal microscopy costaining for the Flag tag on the USP19 and calnexin, an ER marker (Supplemental Figure 2). As expected, USP19-CYT expression was diffuse throughout the cytoplasm, whereas the TMD containing USP19-ER and USP19-ER-CA displayed a mesh-like staining pattern consistent with the ER that colocalized significantly with the ER marker calnexin (Supplemental Figure 2). Overexpressing ER-localized USP19 in C2C12 cells delayed formation and fusion of myotubes, confirming the findings in L6 cells (Figure 3A). Interestingly, the absence of either USP19 catalytic activity or the TMD prevented these effects on cell fusion. We also tested whether these requirements also applied to USP19 regulation of expression of myogenin and myofibrillar proteins. Levels of myogenin (Figure 3B) and MHC and tropomyosin (Figure 3C) are decreased by 40–50% upon USP19-ER overexpression compared with GFP control, but not upon overexpression of the USP19-ER-CA or USP19-CYT variants. Thus catalytic activity and ER localization appear essential for USP19 regulation of muscle cell fusion and expression of myogenin and myofibrillar proteins.

Silencing of USP19-ER but not USP19-CYT increases expression of myofibrillar proteins and myogenin and enhances fusion

To confirm the specific requirement of USP19's ER localization for its ability to modulate myofibrillar proteins, myogenin, and myotube fusion, we tested whether silencing the USP19-ER isoform specifically could reproduce the phenotype observed upon depletion of all USP19 isoforms. Because all available USP19 antibodies recognize both isoforms, the specificity of the ER and CYT small interfering RNA (siRNA) oligonucleotides toward their intended USP19 isoform(s) was confirmed by quantitative real-time PCR (qPCR) using primers directed toward the 3′ end sequences specific for the ER or CYT isoforms (Supplemental Figure 3, A and B). Quantification of total USP19 in transfected cells by Western blotting revealed a >80% suppression of total USP19 levels when targeting both isoforms or the USP19-CYT isoform specifically, and ~10–40% depletion when targeting the USP19-ER isoform specifically, indicating that the major portion of USP19 is located in the cytoplasm (Supplemental Figure 3C). Depletion of all isoforms of USP19 increased myogenin (Figure 4A) and tropomyosin and MHC protein levels (Figure 4B), as previously reported (Sundaram *et al.*, 2009), and enhanced myotube formation and fusion (Figure 4C). Indeed, silencing of the TMD containing USP19-ER isoform was sufficient to reproduce these effects (Figure 4, A–C). In contrast, silencing of the USP19-CYT isoform by more than 80% at the protein level did not significantly alter any of these parameters. These results strongly implicate specifically the USP19-ER isoform in suppressing muscle cell differentiation and indicate that the ER localization of USP19 is essential for its functions in muscle cell differentiation.

USP19 suppresses differentiation-induced UPR signaling

The requirement of USP19 ER localization for its myogenic functions suggested a role for USP19 at the ER. Previous work by Nakanishi and colleagues revealed that a transient induction of ER stress is coincident with the differentiation-dependent appearance of MHC (Nakanishi *et al.*, 2005). This induction of ER stress occurs in a small subpopulation of myoblasts during the early stages of differentiation, can be detected by the appearance of the downstream UPR target gene and transcription factor CHOP, results in apoptosis, and is required for differentiation (Nakanishi *et al.*, 2005, 2007). The transient induction of CHOP was confirmed in our hands by IF in C2C12 cells during differentiation (Figure 5A). We therefore tested whether USP19 modulates this differentiation-dependent CHOP induction and, if so, whether it requires ER localization. Expressing USP19-ER in C2C12 cells attenuated induction of CHOP compared with GFP-expressing control cells (Figure 5A). This effect required enzymatic activity and was not seen with USP19-CYT. Furthermore, silencing of all isoforms of USP19 had the converse effect, producing an approximately twofold increase in the number of CHOP-positive cells over CTL-transfected cells (Figure 5B). Silencing only USP19-ER resulted in a similar increase in the number of CHOP-positive cells, whereas silencing of USP19-CYT did not exert any significant effect (Figure 5B).

Inducing ER stress in USP19-overexpressing muscle cells reverses the defect in myotube fusion

These results suggested that USP19 inhibits muscle cell differentiation by suppressing the differentiation-dependent induction of the UPR during myogenesis. To test this possibility, we evaluated whether the fusion defect observed in muscle cells expressing ER-localized USP19 could be reversed by treatment with thapsigargin (Tg, inhibitor of an ER-specific calcium ATPase), which induces ER

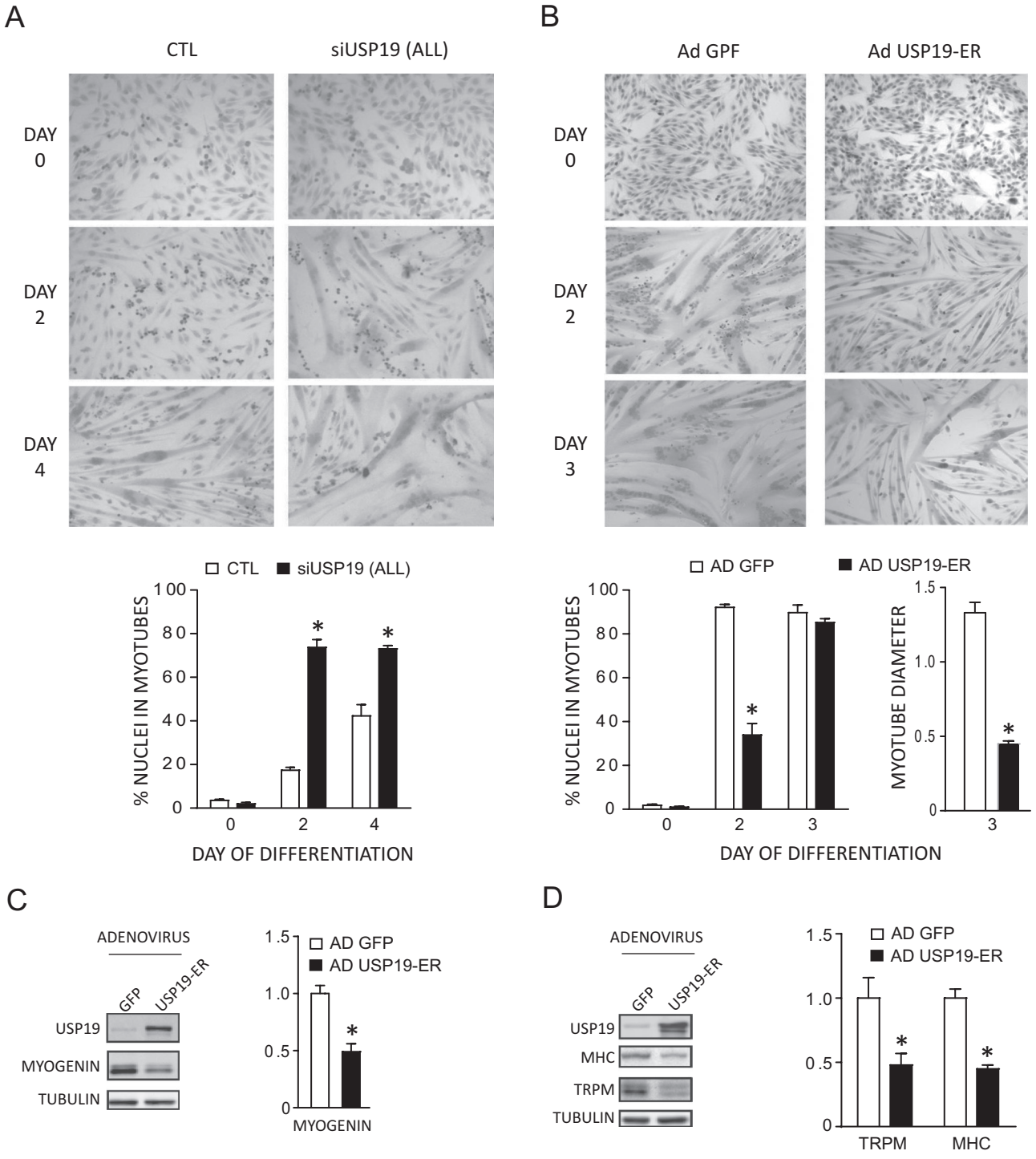

FIGURE 2: USP19 inhibits fusion of L6 myoblasts and suppresses expression of myogenin and major myofibrillar proteins. (A) L6 myoblasts were transfected with control siRNA or USP19 siRNA (ALL) targeting all isoforms and allowed to differentiate for 4 d. Phase-contrast images of cell morphology on days 0, 2, and 4 of differentiation (top). Fusion index for cells transfected with USP19 (ALL) or CTL siRNA (bottom). The fusion index was the proportion of nuclei in myotubes (defined as cells with ≥2 nuclei). *, $p < 0.001$ compared with CTL (two-way ANOVA). (B) L6 myoblasts were infected with adenovirus expressing either GFP control or USP19-ER and allowed to differentiate for 3 d. Phase-contrast images of cell morphology on days 0, 2, and 3 of differentiation (top). Fusion index determined on days 0, 2, and 3 of differentiation and myotube diameter determined on day 3 of differentiation (bottom). *, $p < 0.001$ compared with GFP control (two-way ANOVA). (C and D) L6 myoblasts were infected with adenovirus expressing GFP control or USP19-ER. Cell lysates were prepared 24 h (C) or 48 h (D) after the cells were shifted into differentiation medium. Left, representative Western blots with the indicated antibodies. Right, quantitation from multiple samples of protein expression of myogenin, MHC, and tropomyosin ($n = 3$). Shown are means ± SE. *, $p < 0.05$ compared with GFP (*t* test).

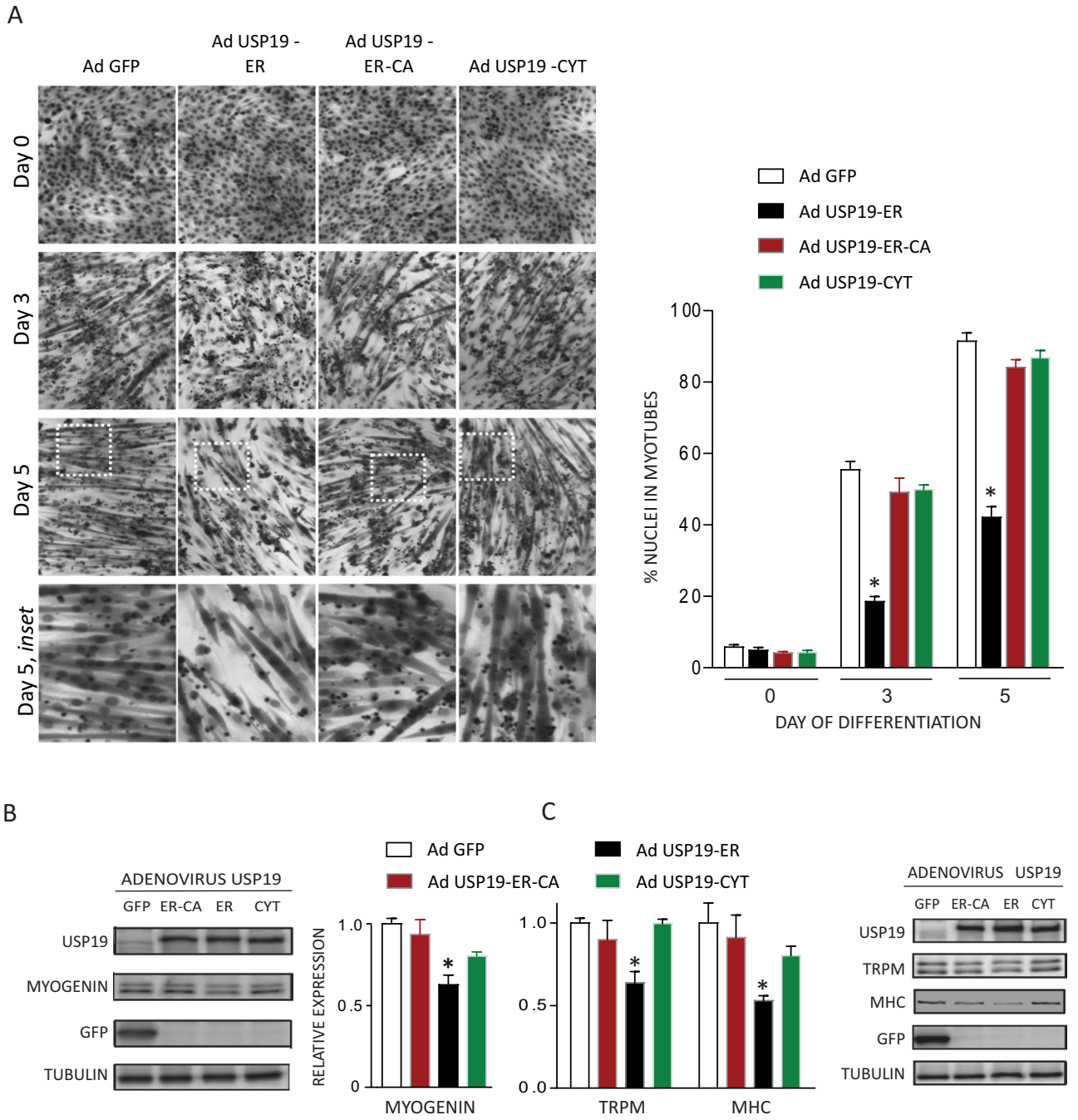

FIGURE 3: USP19 catalytic activity and ER localization are required for modulation of C2C12 differentiation. (A) C2C12 myoblasts were infected with adenovirus expressing either GFP control or USP19-ER, USP19-ER-CA, or USP19-CYT and allowed to differentiate for 5 d. Representative examples of cell morphology on days 0, 3, and 5 of differentiation are shown on the left. The fusion index (right) was determined by counting the nuclei from three randomly selected images and determining the proportion of nuclei in myotubes (defined as cells with ≥2 nuclei). *, $p < 0.001$ compared with GFP (ANOVA). (B and C) C2C12 myoblasts were infected with adenovirus expressing GFP control or USP19-ER, USP19-ER-CA, or USP19-CYT. Cell lysates were prepared 24 h (B) or 48 h (C) after the cells were shifted into differentiation medium and then analyzed by Western blotting with the indicated antibodies. (B) Quantitation of myogenin. (C) MHC and tropomyosin levels ($n \geq 4$). Quantitation displayed as mean ± SE. *, $p < 0.05$ compared with GFP (ANOVA).

stress-dependent activation of the UPR. We used a low concentration (0.1 μM) that was still sufficient to induce CHOP and other markers of the UPR (Supplemental Figure 4). As shown previously (Figure 3), expressing USP19-ER in C2C12 cells significantly delayed myotube formation (Figure 6). Cells infected with adenovirus expressing GFP were ~80% fused after 4 d of differentiation, whereas USP19-ER–expressing cells were only ~50% fused. Both of these fusion indices were higher than in earlier experiments because of growth on gelatin-coated plates (required to decrease the toxicity of Tg), which appears to enhance the rate of fusion. Interestingly,

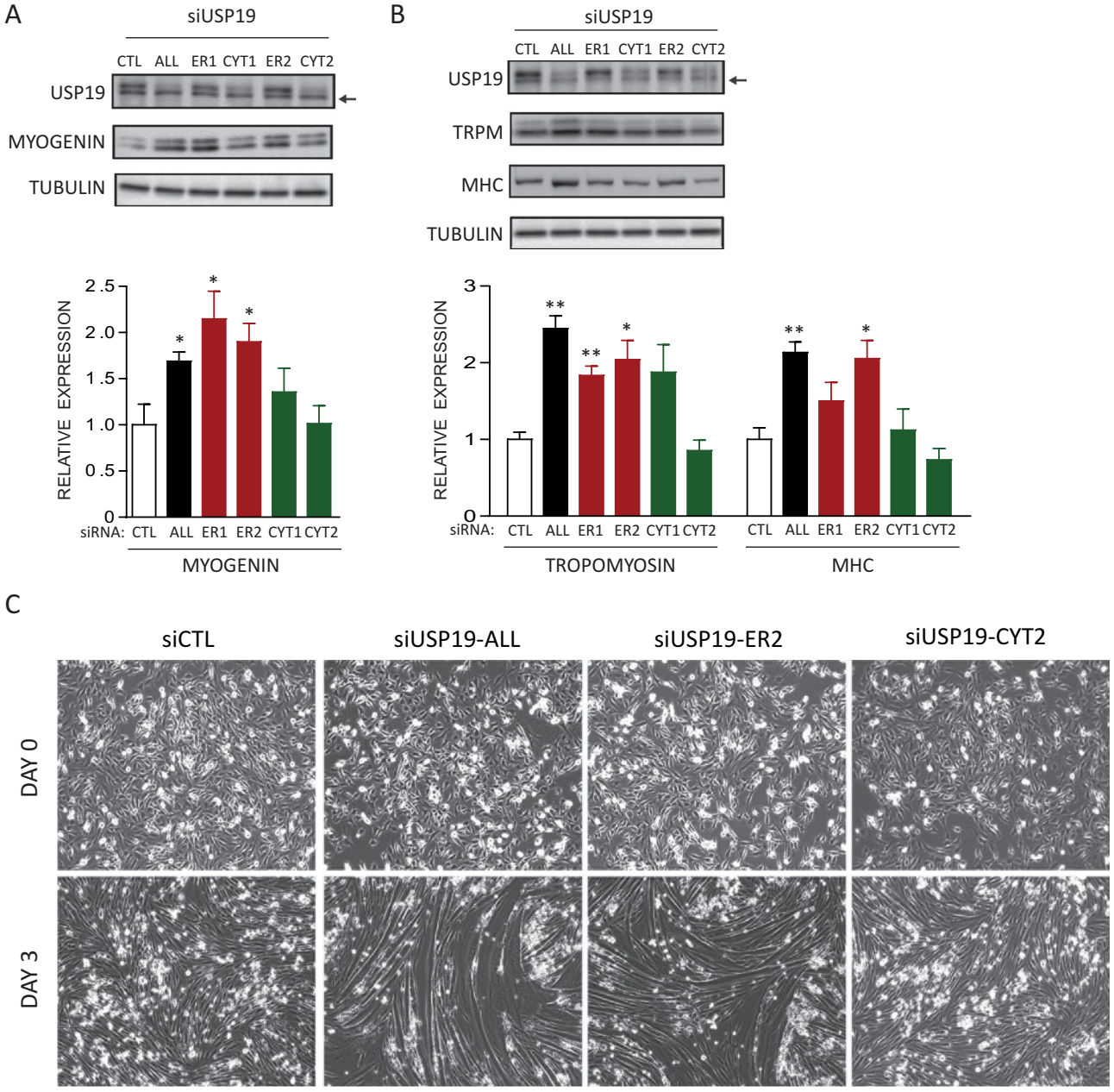

FIGURE 4: Isoform-specific siRNA silencing of USP19-ER but not USP19-CYT increases fusion and expression of myofibrillar proteins and myogenin. L6 myoblasts were transfected with control (CTL) siRNA oligonucleotides or oligonucleotides toward both isoforms of USP19 (ALL), the ER isoform, or the CYT isoform, and differentiated. Cell lysates were prepared 48 h (A) or 72 h (B) after the cells were shifted into differentiation medium and then analyzed by Western blotting (top) with the indicated antibodies. Arrow denotes nonspecific band. Shown below are quantitation of myogenin (A) and MHC and tropomyosin (B) protein levels. Quantitation displayed as mean ± SE ($n \geq 3$). *, $p < 0.05$; **, $p < 0.01$ compared with CTL (*t* test). (C) Representative phase-contrast images of cell morphology and fusion at days 0 and 3 of differentiation (10× magnification).

treating USP19-ER–expressing cells with a low concentration of Tg could reverse the fusion defect (Figure 6). USP19-ER Tg-treated cells were >75% fused at 4 d of differentiation, whereas USP19-ER untreated cells were <50% fused. After 6 d of differentiation, Tg-treated USP19-ER–expressing cells maintained a significantly greater fusion index than untreated USP19-ER–expressing cells. Thus the ability of USP19 to modulate fusion appears to be via its effects on ER stress. The expression of USP19-ER did not modulate Tg induction of CHOP (Supplemental Figure 4), suggesting that there are qualitative and/or quantitative differences in the induction of UPR signaling by chemical inducers (e.g., Tg depletes ER calcium stores) versus differentiation.

USP19 knockout (KO) mice display enhanced muscle regeneration following cardiotoxin-induced muscle injury

To determine whether the effects of silencing USP19 on muscle cell differentiation were relevant in vivo, we induced muscle injury by injecting cardiotoxin into the tibialis anterior (TA) of mice lacking

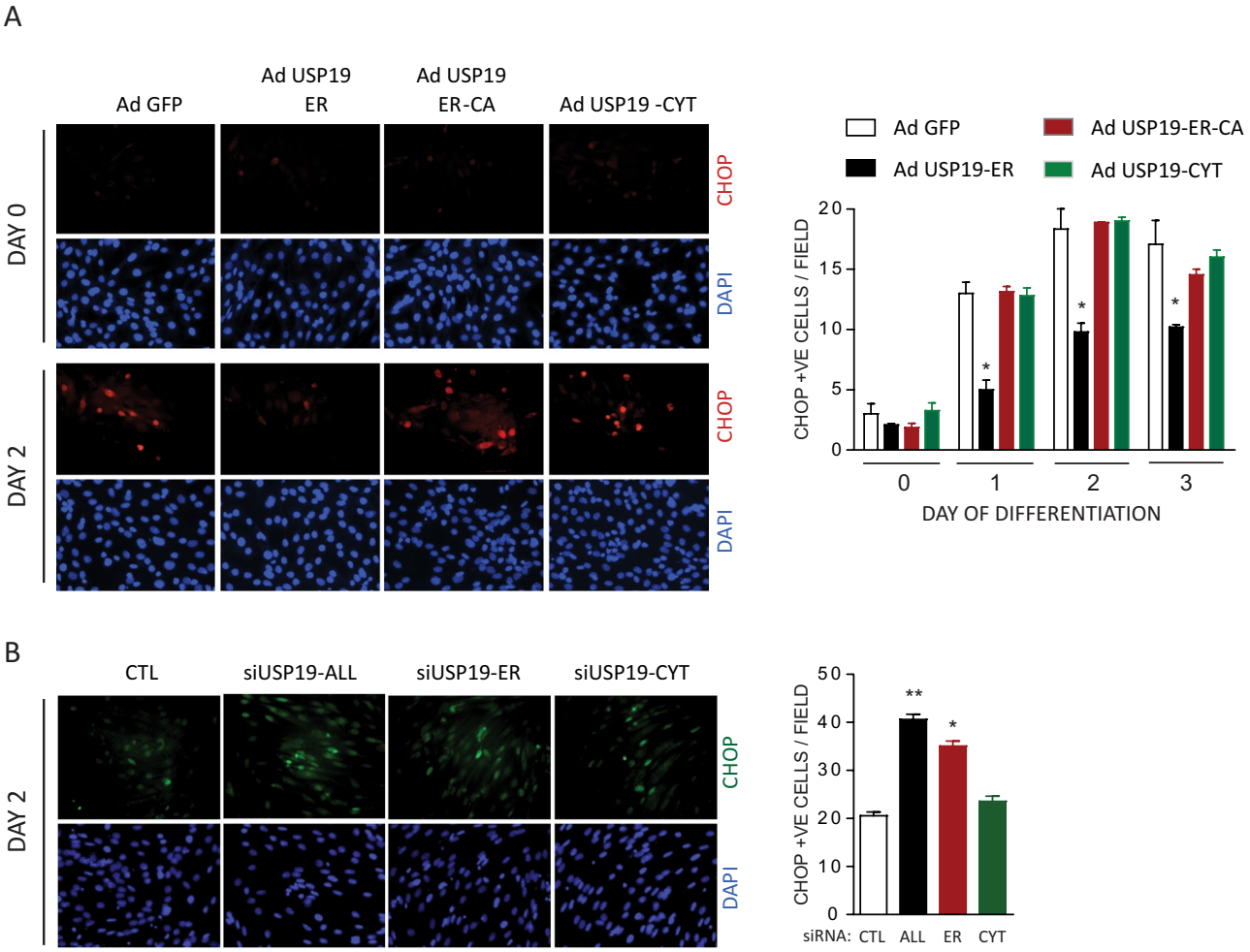

FIGURE 5: USP19 suppresses differentiation-dependent induction of CHOP. C2C12 myoblasts infected with adenovirus expressing GFP control or USP19-ER, USP19-ER-CA, or USP19-CYT were differentiated. After fixation, the cells were probed for CHOP expression using indirect IF and visualized using a fluorescence microscope (40× magnification) on the indicated days of differentiation. (A) Representative images of indirect IF for visualization of CHOP (red) or DAPI (blue) on days 0 and 2 of differentiation (left). Quantification of CHOP-positive cells per view; displayed as average count from five images per group ($n = 3$, right). Shown are means ± SE. *, $p < 0.01$ compared with GFP (two-way ANOVA). (B) L6 myoblasts were transfected with control (CTL) siRNA oligonucleotides or oligonucleotides toward both isoforms of USP19 (ALL), the USP19-ER isoform, or the USP19-CYT isoform, and differentiated for 2 d. Cells were assessed for CHOP induction using indirect IF as in (A), and representative images from day 2 are shown (left). Quantification of CHOP-positive cells per view; displayed as average count from six images per group ($n = 3$, right). Shown are means ± SE. *, $p < 0.05$; **, $p < 0.01$ compared with CTL (two-way ANOVA).

USP19 and wild-type (WT) control littermates. As previously demonstrated (Seale *et al.*, 2000; reviewed in Chargé and Rudnicki, 2004), new myofibers containing centrally located nuclei can be readily identified in the injured muscle at 7 d following injury (Figure 7A). Interestingly, the cross-sectional areas of these fibers were significantly larger in the USP19 KO muscles (Figure 7, B and C), consistent with the hypertrophic phenotype we observed upon silencing of muscle cells (Figure 2A). We also tested whether USP19 regulated muscle gene expression in a manner similar to that observed in cultured muscle cells. Indeed, we observed enhanced expression of myogenin and myosin heavy chain in the muscle lacking USP19 (Figure 7D). Interestingly, the other myogenic regulatory factors were not significantly affected, which was similar to what we had observed previously in muscle cells (Sundaram *et al.*, 2009), indicating that USP19 exerts its effects on a pathway that regulates differentiation specifically at the level of myogenin gene expression (Figure 7D). Interestingly, the expression of CHOP was also up-regulated in the USP19 KO muscle, suggesting that the effects of USP19 seen in muscle cells in vitro were relevant in vivo (Figure 7E). These effects on gene expression were probably underestimated, as only part of the muscle is sufficiently injured to undergo regeneration.

DISCUSSION

In these studies, we have demonstrated very clearly a role for a deubiquitinating enzyme in modulation of muscle cell differentiation. Previous work by us (Sundaram *et al.*, 2009) and others (Ogawa *et al.*, 2011), which primarily used silencing of all isoforms, showed that USP19 reduces fusion of myoblasts and the subsequent induction at a transcriptional level of expression of myogenin and myofibrillar proteins. In this work, we have significantly extended these findings in cultured cells, using both loss and gain of function of the individual USP19 isoforms, and in an in vivo model of myogenesis following

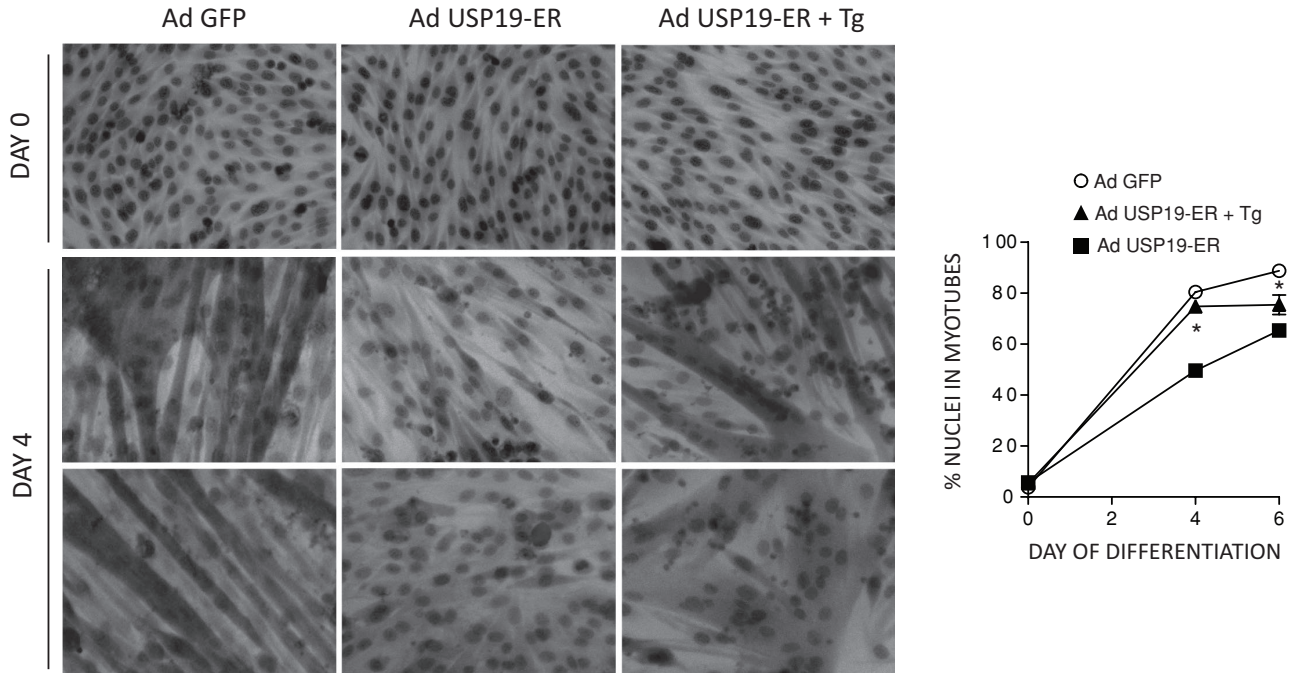

FIGURE 6: Induction of ER stress in myoblasts overexpressing USP19 reverses the defect in myotube fusion. C2C12 myoblasts were seeded on gelatin-coated plates and infected with adenovirus expressing either GFP control or USP19-ER. The day following infection, cells were treated with 0.1 μM Tg in dimethyl sulfoxide (DMSO) or DMSO alone for 30 min and switched into differentiation medium. The cells were fixed, stained with trypan blue, and visualized under a light microscope (10× magnification) on the indicated days. Representative phase-contrast images of cell morphology on days 0 and 4 of differentiation are shown (left). The fusion index was determined by counting the nuclei from three randomly selected images per group and determining the proportion of nuclei in myotubes (defined as cells with ≥2 nuclei; $n \geq 3$, right). *, $p < 0.001$ compared with USP19-ER on the same day (two-way ANOVA).

injury. Furthermore, these effects on differentiation appear due to USP19-mediated down-regulation of UPR signaling. This conclusion is based on several observations. First, USP19 (Figure 5) modulated the expression of CHOP, which had previously been shown to be the key marker of the ER stress response that occurs in only a small fraction of the differentiating myoblasts but is critical for differentiation (Nakanishi *et al*., 2005). Second, the effects of USP19 on CHOP and differentiation (Figures 2–5) were mediated solely and coordinately by the ER-localized isoform and both required its deubiquitinating activity. Finally, reinitiation of the ER stress with Tg, which acts specifically at the ER, was sufficient to largely abrogate the effects of expressing USP19 on muscle cell differentiation (Figure 6). To our knowledge, these findings demonstrate for the first time regulation of UPR signaling by endogenous levels of a deubiquitinating enzyme. The mechanisms by which CHOP expression is modulated by USP19 will require further study. The higher levels of CHOP mRNA seen during regeneration in the USP19 KO muscle suggest that USP19 modulates transcription of CHOP, but modulation of CHOP mRNA stability cannot be excluded. In either case, the effects of USP19 on CHOP induction would likely be indirect, as there is no evidence of USP19 localization in the nucleus, and direct action of USP19 on CHOP would likely stabilize it rather than lower its levels. A recent report demonstrates that overexpressing USP14 in cells expressing mutant Huntington protein results in decreased activation of the ER stress-activated kinase IRE1α and decreased cell toxicity (Hyrskyluoto *et al*., 2014). We attempted to determine whether USP19 modulates specific UPR signaling pathways, but our analyses have been limited by the small percentage of cells that manifest UPR activation during differentiation. In the case of USP19, we have also provided evidence that this modulation of UPR signaling may also occur in vivo during myogenic regeneration in response to muscle injury and that loss of USP19 can lead to a more rapid differentiation and larger myofibers (Figure 7). Thus pharmacological inhibition of USP19 may be a novel approach to enhance recovery from muscle injury.

Previous studies from our group and others reported that USP19 is induced in skeletal muscle atrophying in response to a broad spectrum of catabolic conditions (Combaret *et al*., 2005; Liu *et al*., 2011; Ogawa *et al*., 2012). Our recent studies have demonstrated that mice lacking USP19 do indeed lose less muscle mass and have less myofiber atrophy, indicating that USP19 also plays an essential role in the wasting that occurs in catabolic conditions (unpublished data). Although this effect of USP19 on myofiber growth and atrophy appears distinct from its effect on muscle cell fusion and differentiation, the two processes may be linked. He and colleagues recently described a defect in myoblast fusion in patients with cancer cachexia and demonstrated in tumor-bearing mice that this defect in fusion is required for the muscle wasting that occurs (He *et al*., 2013). Thus inactivation of USP19 may protect against muscle wasting by both increasing myofiber growth and enhancing myoblast fusion with myofibers.

A recent report describing studies in several non–muscle cell lines has concluded that ~80% of endogenous USP19 is cytoplasmically localized but is largely found in the ER when overexpressed, leading the authors to suggest that the expression level of the enzyme affects localization (Lee *et al*., 2014). However, these studies only overexpressed the ER-localized isoform and did not consider the existence of a distinct cytoplasmic isoform. In contrast, our studies recognized the expression of two distinct isoforms with distinctive ER

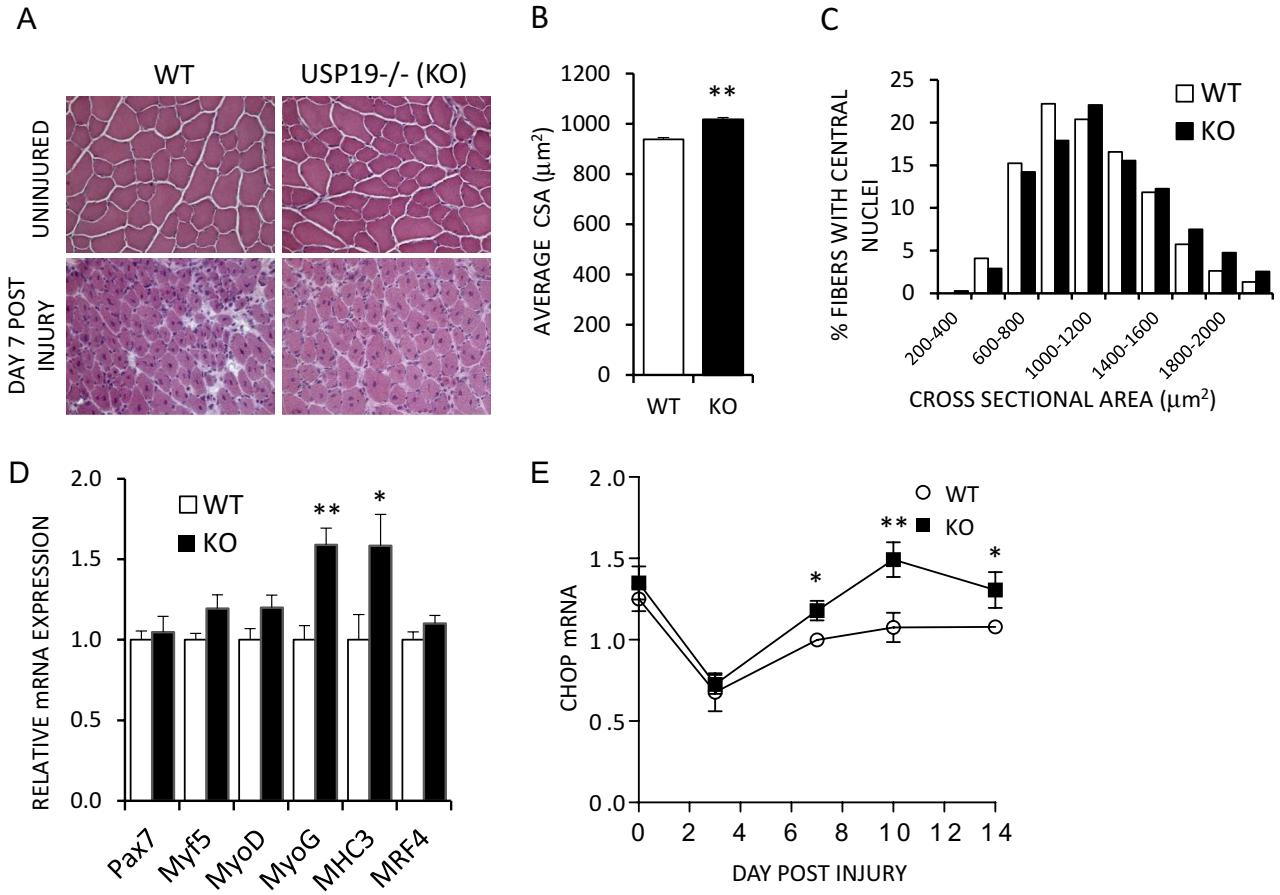

FIGURE 7: Enhanced muscle regeneration following injury in mice lacking USP19. The TA muscles of 8-wk-old USP19 WT and KO mice were injured with cardiotoxin and allowed to regenerate for 7 d. (A) Representative hematoxylin and eosin stain of TA muscles from USP19 WT and KO mice uninjured or at 7 d postinjury. (B and C) Cross-sectional areas of myofibers with centrally located nuclei at 7 d postinjury represented as average cross-sectional area (B) or distribution of fiber size (C). Fibers from 14 animals per genotype were quantified ($n = 2500$). *, $p < 0.05$. (D and E) Relative mRNA expression of myogenic genes (D) and CHOP (E) ($n = 14$). Shown are means ± SE. *, $p < 0.05$; **, $p < 0.01$.

and cytoplasmic localizations. We found that the cytoplasmic isoform is more abundant, explaining the proportions in subcellular distribution of endogenous enzyme observed by Lee and colleagues. Although found at lower levels, the ER-localized form is shown here to be clearly the isoform that is both sufficient and necessary for USP19's effects on myoblast fusion and expression of myofibrillar proteins. A number of reports have suggested that deubiquitinating enzymes have functions that are not dependent on catalytic activity (e.g., Mei *et al.*, 2011; Altun *et al.*, 2012). In contrast, our studies have clearly demonstrated that USP19 catalytic activity is essential for its effects on differentiation and argue that USP19 is deubiquitinating an ER-localized protein that represses the ER stress response. Such a substrate remains to be identified at this time.

Our studies have also revealed for the first time that USP19 is itself regulated during differentiation. USP19 mRNA was induced three- to fourfold during differentiation. Notably, levels of USP19 protein increased by only 1.5-fold, indicating that there is posttranscriptional regulation of expression of USP19 during differentiation. Because USP19 inhibits differentiation, it was somewhat surprising to observe its induction during differentiation. Perhaps its role is to limit myofiber formation to an optimal degree of myoblast fusion. In addition, the induction of USP19 mRNA was largely due to induction of the cytoplasmic form of USP19. Indeed, at days 1 and 2, when the effects of modulating USP19 on fusion were very evident, there was no detectable change in expression of the USP19-ER mRNA. Possibly USP19 activity is modified posttranscriptionally, or the relevant substrates involved in this process become available to the enzyme at this time.

In summary, we have identified two important, linked functions for USP19: modulating muscle cell differentiation and the UPR. The involvement of the latter in many pathological conditions suggests that tuning USP19 activity could be a new approach to treatment of these conditions as well as for muscle wasting.

MATERIALS AND METHODS

Cell culture, transfection, and adenoviral transduction

L6 rat myoblasts (Amira Klip, University of Toronto) or C2C12 mouse myoblasts (American Type Culture Collection, Manassas, VA) were cultured in α-MEM or DMEM (Gibco, Grand Island, NY), respectively, supplemented with 10% fetal bovine serum (FBS) and 1% penicillin/streptomycin (growth medium) at 37°C with 5% CO_2. Typically, cells were plated at a density (~150,000 cells/well in a six-well plate) that would result in 75–80% confluence the following day. Cells were differentiated in α-MEM or DMEM supplemented with 2% FBS and 1% penicillin/streptomycin (differentiation medium), and the medium was replaced every 2 d.

For siRNA transfection, L6 cells at ~75–80% confluence were transfected with 25 nM oligonucleotides (IDT; see Supplemental Table 1 for sequences) using Lipofectamine and Plus Reagent (Invitrogen) and following the manufacturer's protocol. Three hours after transfection, the transfection mixture was supplemented with an equal volume of α-MEM containing 20% FBS. The next day, the medium was replaced with differentiation medium.

Recombinant adenovirus expressing GFP, Flag-tagged rat USP19-ER, USP19-CYT, or USP19-ER-CA (catalytically inactive USP19 in which Cys-545 was mutated to Ala) was generated using AdEasy XL adenoviral vector system (Stratagene). The coding sequence was derived from the rat sequence and contained silent mutations rendering it resistant to the #7 siRNA oligo that targets all isoforms (Lu *et al.*, 2009). For generation of USP19-CYT, the non-TMD isoform, cDNA was prepared from rat testis RNA using the High Capacity cDNA Reverse Transcriptase kit (Applied Biosystems, Waltham, MA). The non-TMD region of USP19 was amplified from the cDNA by PCR using the following as primers: forward 5′- CAC TAC GGA GGC ATG ATC GG -3′ and reverse 5′- GAT TCT GCA GTT TGT CTA CGG ACC TGC TAA TCG ACC -3′. The forward primer is located in a region common to both isoforms and upstream of an *Acc*I restriction site. The reverse primer is complementary to the end of the coding region specific to the cytoplasmic isoform and includes an *Acc*I site distal to the stop codon. The amplified fragment was cloned into the pGEM-T vector (Promega). The resulting plasmid was digested with *Acc*I, and the fragment ligated into a pBluescript plasmid containing rat USP19, which had also been digested with *Acc*I in order to remove its TMD domain.

Viruses were amplified in AD-293 cells and collected as instructed in the protocol. Viral titer was measured by plaque assay using agarose overlay or by the AdEasy Viral Titer kit (Stratagene). For adenovirus infection, L6 or C2C12 cells at 75–80% confluence in six-well plates were exposed to 1 ml of growth medium containing virus at multiplicity of infection (MOI) of ~80–120 to achieve similar levels of overexpression. Two hours later, 1 ml of growth medium was added to each well, and the cells were incubated for a further 18 h. Medium was then replaced with differentiation medium.

For studies involving exposure to Tg, C2C12 myoblasts (30,000) were seeded in 24-well plates precoated with 0.2 mg/ml gelatin (to enhance adhesion) and incubated overnight in growth medium. The next day, cells were infected with adenovirus as outlined earlier. The following day, when cells were fully confluent, the infection medium was removed and cells were washed once in phosphate-buffered saline (PBS) and then treated with 0.1 μM Tg in growth medium for 30 min to induce mild ER stress. For these studies, differentiation was induced by changing the medium to DMEM supplemented with 2% horse serum and 1 μg/ml insulin (Nakanishi *et al.*, 2005).

Determination of fusion index

For quantifying fusion, cells were washed twice with PBS and fixed in 95% ethanol for 15 min. Following rinsing with PBS and staining in 0.2% trypan blue solution (Sigma-Aldrich) for 15 min, the cells were washed twice with PBS and overlaid with glycerol. The stained cells were visualized using a light microscope at 10× magnification. Nuclei were counted manually from three randomly chosen fields per experimental group (a total of 2000–3000 nuclei were counted for each experimental group). The fusion index was determined by calculating the percentage of total nuclei found in myotubes, which were defined as cells with two or more nuclei. For each protocol, at least one of the experiments was done with the observer blinded to treatment conditions, and similar and statistically significant results were obtained.

RNA analysis by qPCR

RNA was isolated by solubilizing cells in 4 M guanidinium isothiocyanate; this was followed by phenol-chloroform extraction (Chomczynski and Sacchi, 1987). Quantification was done using a NanoDrop LITE spectrophotometer (Thermo Fisher Scientific, Waltham, MA). cDNA was synthesized using 1 μg of RNA and the High-Capacity cDNA Reverse Transcriptase Kit (Applied Biosystems). qPCR analysis was performed using SYBR-Green Reagents and a ViiA7 qPCR analyzer (Applied Biosystems) (see Supplemental Table 2 for primer sequences). Glyceraldehyde 3-phosphate dehydrogenase or porphobilinogen deaminase was used as a control gene in qPCR to normalize for variations in loading. Differences in target gene expression were determined using the ΔΔ-CT method (Livak and Schmittgen, 2001).

Western blotting

Cells were washed once in PBS and lysed in 50 mM Tris (pH 7.5), 2% SDS; this was followed by scraping to collect the cell lysate. Following repeated aspiration of the lysate using a 23-gauge 1-ml insulin syringe to shear the DNA, the lysate was clarified on a tabletop microcentrifuge (Beckman) at 12,500 rpm for 15 min. The protein concentrations of the samples were determined by the BCA Micro Protein Assay (Thermo Fisher Scientific). Samples were subjected to SDS–PAGE, and the proteins were transferred onto 0.45-μm nitrocellulose membranes for Western blotting. Membranes were probed with primary antibodies (Supplemental Table 3) followed by either horseradish peroxidase–conjugated secondary antibodies and ECL (Thermo Fisher Scientific) with the chemiluminescent signals imaged using a cooled digital camera (Versadoc; BioRad) or by a radioiodinated secondary antibody with the radioactive signals detected by exposure to a phosphorimager screen and analysis with a phosphorimager (Typhoon; GE Healthcare). The latter was used to avoid signal saturation during fine quantitation. Protein signals were normalized to tubulin on the same blot to control for variations in loading and membrane transfer.

Immunofluorescence

C2C12 myoblasts (60,000) were seeded on glass coverslips in 24-well plates and incubated overnight in growth medium. The next day, cells were infected with adenovirus and then induced to differentiate as described under *Cell culture, transfection, and adenoviral transduction*. For analysis, cells were rinsed once in DMEM containing 10 mM HEPES and then fixed in 4% paraformaldehyde for 20 min. The cells were then rinsed twice as described under *Cell culture, transfection, and adenoviral transduction*; this was followed by a 1-h incubation in DMEM containing 10 mM HEPES, 2% FBS, 0.1% Triton X-100, and primary antibody (Supplemental Table 3). Following three washes in DMEM containing 10 mM HEPES, the cells were incubated for 1 h in DMEM containing 10 mM HEPES, 2% FBS, and fluorescently labeled secondary antibody. The cells were washed three times, incubated for 10 min with 4′,6-diamidino-2-phenylindole (DAPI) in PBS, rinsed two times with distilled water, and mounted on glass slides using ProLong Gold anti-fade reagent (Invitrogen, Carlsbad, CA). Slides were visualized as described using an Axio fluorescence microscope (40× magnification; Zeiss, Oberkochen, Germany) and MetaMorph imaging software.

In vivo muscle regeneration induced by cardiotoxin injury

All animal studies were approved by the McGill University Animal Care Committee. Cardiotoxin (CTX) from *Naja mossambica mossambica* (Sigma) was prepared as a 10 μM solution in sterile saline.

USP19 WT and KO mice (8 wk old; unpublished data) were anesthetized, and the hind legs were shaved and cleaned. Each TA muscle was injected with 50 µl CTX with a 28-gauge insulin syringe. When the animals were killed, one TA muscle was homogenized in 4 M guanidinium isothiocyanate, followed by phenol-chloroform extraction to isolate RNA, and the other was flash-frozen in isopentane for cryosectioning. cDNA was prepared with 750 ng RNA, and RT-PCR analysis was performed as described under *RNA analysis by qPCR*. TA muscles were sectioned at the midbelly in 9-µm sections and stained with hematoxylin and eosin. For cross-sectional area analysis, myofibers were visualized with anti-dystrophin antibody to identify the cell membrane and fluorescently labeled goat anti-mouse FITC (Sigma, St. Louis, MO) antibodies. Slides were visualized as described under *Immunofluorescence* but with 10× magnification. Approximately 200 myofibers with centrally located nuclei were analyzed per animal using ImageJ software.

ACKNOWLEDGMENTS

This work was supported by a grant from the Canadian Institutes of Health Research (MOP 82734) to S.S.W. A.V.C. is supported by the Catherine McLaughlin Hakim Chair.

REFERENCES

Allen DL, Linderman JK, Roy RR, Bigbee AJ, Grindeland RE, Mukku V, Edgerton VR (1997). Apoptosis: a mechanism contributing to remodeling of skeletal muscle in response to hindlimb unweighting. Am J Physiol 273, C579–C587.

Altun M, Zhao B, Velasco K, Liu H, Hassink G, Paschke J, Pereira T, Lindsten K (2012). Ubiquitin-specific protease 19 (USP19) regulates hypoxia-inducible factor 1α (HIF-1α) during hypoxia. J Biol Chem 287, 1962–1969.

Bentzinger CF, Wang YX, Rudnicki MA (2012). Building muscle: molecular regulation of myogenesis. Cold Spring Harbor Perspect Biol 4, a008342.

Bodine SC, Latres E, Baumhueter S, Lai VK, Nunez L, Clarke BA, Poueymirou WT, Panaro FJ, Na E, Dharmarajan K, *et al*. (2001). Identification of ubiquitin ligases required for skeletal muscle atrophy. Science 294, 1704–1708.

Boutet SC, Biressi S, Iori K, Natu V, Rando TA (2010). Taf1 regulates Pax3 protein by monoubiquitination in skeletal muscle progenitors. Mol Cell 40, 749–761.

Brooks NE, Myburgh KH (2014). Skeletal muscle wasting with disuse atrophy is multi-dimensional: the response and interaction of myonuclei, satellite cells and signaling pathways. Frontiers Physiol 5, 99.

Chargé SBP, Rudnicki MA (2004). Cellular and molecular regulation of muscle regeneration. Physiol Rev 84, 209–238.

Chomczynski P, Sacchi N (1987). Single-step method of RNA isolation by acid guanidinium thiocyanate-phenol-chloroform extraction. Anal Biochem 162, 156–159.

Combaret L, Adegoke OA, Bedard N, Baracos V, Attaix D, Wing SS (2005). USP19 is a ubiquitin-specific protease regulated in rat skeletal muscle during catabolic states. Am J Physiol Endocrinol Metab 288, E693–E700.

Gomes MD, Lecker SH, Jagoe RT, Navon A, Goldberg AL (2001). Atrogin-1, a muscle-specific F-box protein highly expressed during muscle atrophy. Proc Natl Acad Sci USA 98, 14440–14445.

Hassink GC, Zhao B, Sompallae R, Altun M, Gastaldello S, Zinin NV, Masucci MG, Lindsten K (2009). The ER-resident ubiquitin-specific protease 19 participates in the UPR and rescues ERAD substrates. EMBO Rep 10, 755–761.

Hasty P, Bradley A, Morris JH, Edmondson DG, Venuti JM, Olson EN, Klein WH (1993). Muscle deficiency and neonatal death in mice with a targeted mutation in the myogenin gene. Nature 364, 501–506.

He WA, Berardi E, Cardillo VM, Acharyya S, Aulino P, Thomas-Ahner J, Wang J, Bloomston M, Muscarella P, Nau P, *et al*. (2013). NF-κB-mediated Pax7 dysregulation in the muscle microenvironment promotes cancer cachexia. J Clin Invest 123, 4821–4835.

Hyrskyluoto A, Bruelle C, Lundh SH, Do HT, Kivinen J, Rappou E, Reijonen S, Waltimo T, Petersen A, Lindholm D, Korhonen L (2014). Ubiquitin-specific protease-14 reduces cellular aggregates and protects against mutant huntingtin-induced cell degeneration: involvement of the proteasome and ER stress-activated kinase IRE1alpha. Hum Mol Genet 23, 5928–5939.

Jogo M, Shiraishi S, Tamura TA (2009). Identification of MAFbx as a myogenin-engaged F-box protein in SCF ubiquitin ligase. FEBS Lett 583, 2715–2719.

Lee JG, Kim W, Gygi S, Ye Y (2014). Characterization of the deubiquitinating activity of USP19 and its role in endoplasmic reticulum-associated degradation. J Biol Chem 289, 3510–3517.

Liu Q, Xu WG, Luo Y, Han FF, Yao XH, Yang TY, Zhang Y, Pi WF, Guo XJ (2011). Cigarette smoke-induced skeletal muscle atrophy is associated with up-regulation of USP-19 via p38 and ERK MAPKs. J Cell Biochem 112, 2307–2316.

Livak KJ, Schmittgen TD (2001). Analysis of relative gene expression data using real-time quantitative PCR and the $2^{-\Delta\Delta C_T}$ method. Methods 25, 402–408.

Lu Y, Adegoke OA, Nepveu A, Nakayama KI, Bedard N, Cheng D, Peng J, Wing SS (2009). USP19 deubiquitinating enzyme supports cell proliferation by stabilizing KPC1, a ubiquitin ligase for p27Kip1. Mol Cell Biol 29, 547–558.

Mei Y, Hahn AA, Hu S, Yang X (2011). The USP19 deubiquitinase regulates the stability of c-IAP1 and c-IAP2. J Biol Chem 286, 35380–35387.

Nakamura N, Harada K, Kato M, Hirose S (2014). Ubiquitin-specific protease 19 regulates the stability of the E3 ubiquitin ligase MARCH6. Exp Cell Res 328, 207–216.

Nakanishi K, Dohmae N, Morishima N (2007). Endoplasmic reticulum stress increases myofiber formation in vitro. FASEB J 21, 2994–3003.

Nakanishi K, Sudo T, Morishima N (2005). Endoplasmic reticulum stress signaling transmitted by ATF6 mediates apoptosis during muscle development. J Cell Biol 169, 555–560.

Ogawa M, Kariya Y, Kitakaze T, Yamaji R, Harada N, Sakamoto T, Hosotani K, Nakano Y, Inui H (2012). The preventive effect of beta-carotene on denervation-induced soleus muscle atrophy in mice. Br J Nutr 1–10.

Ogawa M, Yamaji R, Higashimura Y, Harada N, Ashida H, Nakano Y, Inui H (2011). 17β-estradiol represses myogenic differentiation by increasing ubiquitin-specific peptidase 19 through estrogen receptor α. J Biol Chem 286, 41455–41465.

Rudnicki MA, Schnegelsberg PN, Stead RH, Braun T, Arnold HH, Jaenisch R (1993). MyoD or Myf-5 is required for the formation of skeletal muscle. Cell 75, 1351–1359.

Schiaffino S, Dyar KA, Ciciliot S, Blaauw B, Sandri M (2013). Mechanisms regulating skeletal muscle growth and atrophy. FEBS J 280, 4294–4314.

Seale P, Sabourin LA, Girgis-Gabardo A, Mansouri A, Gruss P, Rudnicki MA (2000). Pax7 is required for the specification of myogenic satellite cells. Cell 102, 777–786.

Siu PM (2009). Muscle apoptotic response to denervation, disuse, and aging. Med Sci Sports Exercise 41, 1876–1886.

Sundaram P, Pang Z, Miao M, Yu L, Wing SS (2009). USP19-deubiquitinating enzyme regulates levels of major myofibrillar proteins in L6 muscle cells. Am J Physiol Endocrinol Metab 297, E1283–E1290.

Tintignac LA, Lagirand J, Batonnet S, Sirri V, Leibovitch MP, Leibovitch SA (2005). Degradation of MyoD mediated by the SCF (MAFbx) ubiquitin ligase. J Biol Chem 280, 2847–2856.